

Stepwise Synthesis of Giant Unilamellar Vesicles on a Microfluidic Assembly Line

Sandro Matosevic and Brian M. Paegel*

Department of Chemistry, The Scripps Research Institute, Jupiter, Florida 33458, United States

Supporting Information

ABSTRACT: Among the molecular milieu of the cell, the membrane bilayer stands out as a complex and elusive synthetic target. We report a microfluidic assembly line that produces uniform cellular compartments from droplet, lipid, and oil/water interface starting materials. Droplets form in a lipid-containing oil flow and travel to a junction where the confluence of oil and extracellular aqueous media establishes a flow-patterned interface that is both stable and reproducible. A triangular post mediates phase transfer bilayer assembly by deflecting droplets from oil, through the interface, and into the extracellular aqueous phase to yield a continuous stream of unilamellar phospholipid vesicles with uniform and tunable size. The size of the droplet precursor dictates vesicle size, encapsulation of small-molecule cargo is highly efficient, and the single bilayer promotes functional insertion of a bacterial transmembrane pore.

In pursuit of a total synthesis of the cell, chemical and enzymatic routes to small-molecule metabolites, oligonucleotides, genes, peptides, and proteins abound, but there are no elegant synthetic strategies for accessing the lipid bilayer envelope. Studies of compartmentalized metabolism and replication^{1–3} must instead rely on bulk approaches such as lipid-film hydration⁴ and electroformation⁵ to construct the centerpiece membrane bilayer, which is afforded in heterogeneous mixtures of multilamellar structures with inefficient encapsulation and an inscrutable mechanism of assembly. Other studies concerning membrane protein biophysics⁶ have abandoned vesicle synthesis altogether in favor of planar supported lipid bilayers,⁷ which provide the needed bilayer structure but neither the curvature nor the spherical continuity of cellular membranes. Here we report a microfluidic assembly line that produces giant unilamellar vesicles with uniform, tunable size and efficient encapsulation.

Assembly-line vesicle production (Figure 1) begins with flow-focusing⁸ generation of uniform and programmable lipid-stabilized droplets that contain the cytoplasmic aqueous interior. The droplets in oil travel to a junction where they merge and coflow with the extracellular aqueous input. From the combination of multiphase flow⁹ and laminar flow patterning,^{10,11} a lipid-stabilized oil/water interface forms between the droplet flow and the extracellular aqueous flow. Finally, a triangular guide post mediates phase transfer of the droplets from the oil flow through the interface and into the extracellular aqueous flow. During phase transfer, lipids residing at the interface are deposited on the droplet-adsorbed lipids, forming the outer and inner leaflets of the nascent membrane bilayer.¹²

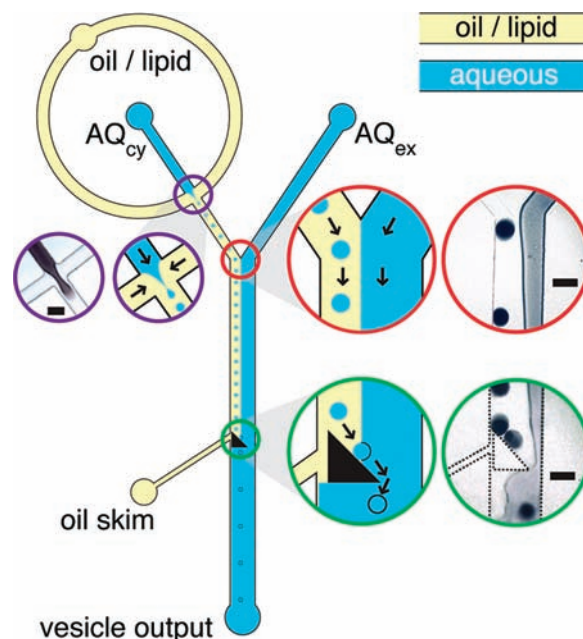


Figure 1. Circuit schematic and operation of the microfluidic assembly line. The oil/lipid input is introduced at the top left, focusing the cytoplasmic aqueous input (AQ_{cy}) to generate uniform, lipid-stabilized droplets (purple insets). The droplet flow merges with an extracellular aqueous input (AQ_{ex}) to form a lipid-stabilized oil/water interface adjacent to the droplet flow (red insets). Droplets impinge on a triangular post in the center of the channel, where the oil flow is skimmed while droplets are deflected along the hypotenuse of the post and traverse the interface, completing the lipid bilayer to form a unilamellar vesicle (green insets). Arrows indicate the flow field. (Micrograph scale bar = 100 μm .)

Vesicles collected from the device exhibited excellent integrity. The vesicles retained both macromolecular (dextran) and small-molecule (fluorescein dye) cargo, as observed during epifluorescence microscopy imaging, and no oil contamination or oil-induced defects of the bilayer were visible in high-resolution differential interference contrast (DIC) images (Figure 2A). Treatment with *Staphylococcus aureus* α -hemolysin, a bacterial transmembrane pore-forming toxin, selectively permeabilized the membrane to fluorescein, demonstrating that the bilayer mediates correct insertion, folding, and function of a transmembrane protein complex (Figure 2B). Complete discharge of fluorescein verified the absence of internal lamellae that would

Received: October 19, 2010

Published: February 10, 2011

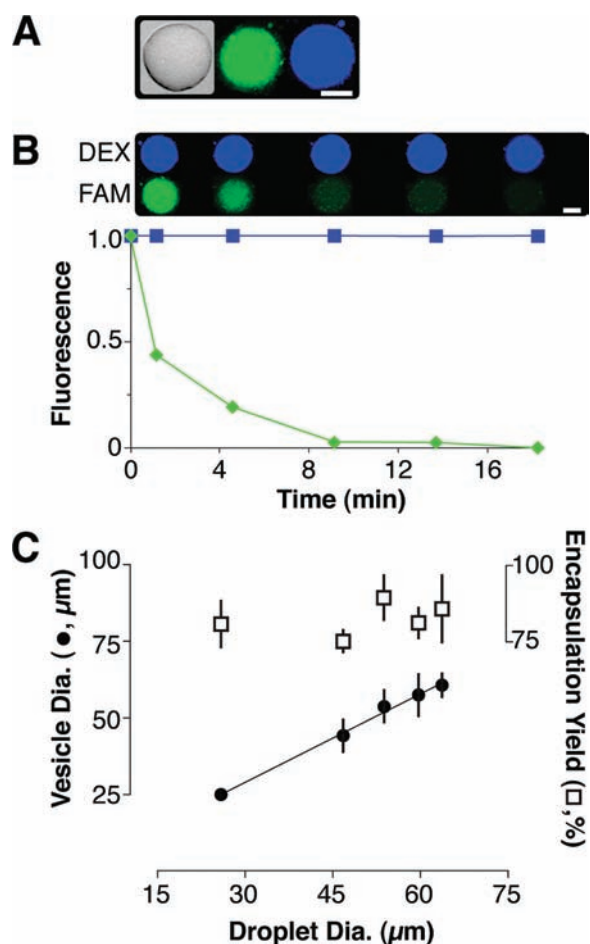


Figure 2. Analysis of assembly line vesicle products. (A) Droplets loaded with blue fluorescent dextran macromolecular cargo (DEX, 10 kDa) and fluorescein dye small-molecule cargo (FAM, 332 Da) were formed in the dodecane/1,2-dioleoyl-*sn*-glycero-3-phosphatidylcholine oil phase and assembled into vesicles. The resultant vesicles were imaged in bright-field DIC mode (left) and in epifluorescence mode using a fluorescein filter (center) or Cascade Blue filter (right). Scale = 10 μm . (B) Vesicles were treated with *S. aureus* hemolysin toxin to test vesicular integrity and lamellarity. Vesicles were stable for hours prior to hemolysin treatment. Post treatment, selective membrane permeabilization was observed in two-color confocal fluorescence microscopy time courses that demonstrated fluorescein leakage and dextran retention for a 20- μm -diameter vesicle. Scale = 10 μm . (C) Vesicle size and encapsulation yield data plotted for each size of droplet starting material. The vesicle product size was linearly correlated with the droplet precursor size ($m = 0.96$, $R^2 = 0.993$), while the encapsulation yield was independent of the precursor size.

otherwise remain unexposed to the exogenous pore and retain fluorescein.

Deconstruction of vesicle assembly into discrete fluidic steps permitted quantitative probing of each chemical step in the process. For example, the product vesicle size was found to correlate linearly with the size of the droplet intermediate (Figure 2C). Furthermore, the cargo concentration (as calculated by in situ quantitation of fluorescent material in the vesicle product) divided by that of the droplet just prior to phase transfer gives the encapsulation yield for a single vesicle assembly event. The encapsulation yield was high (83%) in comparison with bulk strategies and independent of droplet size. Cargo that was not encapsulated during vesicle assembly was lost during droplet

transfer from the oil phase to the extracellular aqueous phase, as observed in high-speed documentation of the transfer process.

The controlled synthesis of cell-sized vesicles has been a long-standing challenge since the discovery that lipids self-assemble into these structures in bulk. Microfluidic technology can rein in the intrinsic chaos of bulk assembly procedures, such as mixing, compartment formation, solvent evaporation, and interface formation. For example, laminar-flow focusing of lipid-containing alcohol and aqueous phases systematizes the mixing step of lipid-film hydration to promote the controlled formation of uniform submicrometer unilamellar vesicles.¹³ Droplet jetting through a lipid bilayer produces uniform giant unilamellar vesicles,^{14–16} and other configurations have achieved limited size control over tens of product vesicles.¹⁷ Each approach elegantly circumvents some of the vexing drawbacks of bulk vesicle assembly, but simultaneous control over size, encapsulation efficiency, and lamellarity at the cellular scale remains challenging.

The assembly-line approach described here accesses cellular compartments that are produced continuously with efficient encapsulation of small-molecule cargo and tunable over the range of eukaryotic cell sizes. Vesicle diameters explored using this microchip architecture ranged from 20 to 70 μm . Assembly of smaller vesicles is limited by the challenge of generating 1- μm -scale droplets¹⁸ and guiding smaller droplets onto the triangular guide post. Smaller droplets are more easily lost in the oil-skim channel. Assembly of larger vesicles is limited solely by the dimensions of the channel. The width of the oil flow must be such that droplets are entirely sheathed in oil until they transit the interface on the triangular guide post. If the droplet is so large that it prematurely contacts the interface, fusion occurs and the droplet is lost into the extracellular aqueous flow. These factors also influence the yield. The current circuit architecture assembles vesicles at 5% of the droplet generation rate for mid-sized vesicles but drops off to 1% and lower as the droplet size falls outside this range. Expanding the vesicle size range, lipid substrate scope, and assembly yield will rely on larger channel widths and less disruptive modes of transferring droplets between phases. These are the subjects of ongoing investigations in our laboratory.

This assembly-line strategy represents a dramatic leap forward in systematic control over phospholipid vesicle preparation because each step is completely parametrized and reproducible. The compartment size is controlled by the relative flow rates of the oil and cytoplasmic aqueous phases during droplet formation; also, the interface used during each bilayer formation event is continuously renewed, so each droplet encounters a fresh interface that has been stabilized for a defined time. With this approach, cell-membrane assembly is now a computer-programmed reaction, like peptide and oligonucleotide synthesis, but specified in lipid/oil and aqueous inputs, flow rates, and channel geometry.

■ ASSOCIATED CONTENT

S Supporting Information. Materials and methods, example data on size dependence and encapsulation yield, hemolysin toxin leakage assay schematic, photobleaching and vesicle stability data, vesicle diameter variance data, droplet/interface movie (MPG), and high-speed phase transfer movie (MPG). This material is available free of charge via the Internet at <http://pubs.acs.org>.

■ AUTHOR INFORMATION

Corresponding Author
briandna@scripps.edu

ACKNOWLEDGMENT

This work was supported by an NIH Pathway to Independence Career Development Award to B.M.P. (GM083155).

REFERENCES

- (1) Noireaux, V.; Libchaber, A. *Proc. Natl. Acad. Sci. U.S.A.* **2004**, *101*, 17669–17674.
- (2) Mansy, S. S.; Schrum, J. P.; Krishnamurthy, M.; Tobe, S.; Treco, D. A.; Szostak, J. W. *Nature* **2008**, *454*, 122–126.
- (3) Long, M. S.; Jones, C. D.; Helfrich, M. R.; Mangeney-Slavin, L. K.; Keating, C. D. *Proc. Natl. Acad. Sci. U.S.A.* **2005**, *102*, 5920–5925.
- (4) Bangham, A. D.; Standish, M. M.; Watkins, J. C. *J. Mol. Biol.* **1965**, *13*, 238–252.
- (5) Angelova, M. I.; Dimitrov, D. S. *Faraday Discuss.* **1986**, *81*, 303–311.
- (6) Loose, M.; Fischer-Friedrich, E.; Ries, J.; Kruse, K.; Schwille, P. *Science* **2008**, *320*, 789–792.
- (7) Brian, A. A.; McConnell, H. M. *Proc. Natl. Acad. Sci. U.S.A.* **1984**, *81*, 6159–6163.
- (8) Anna, S. L.; Bontoux, N.; Stone, H. A. *Appl. Phys. Lett.* **2003**, *82*, 364–366.
- (9) Tokeshi, M.; Minagawa, T.; Kitamori, T. *Anal. Chem.* **2000**, *72*, 1711–1714.
- (10) Kenis, P. J. A.; Ismagilov, R. F.; Whitesides, G. M. *Science* **1999**, *285*, 83–85.
- (11) Zhao, B.; Moore, J. S.; Beebe, D. J. *Science* **2001**, *291*, 1023–1026.
- (12) Pautot, S.; Frisken, B. J.; Weitz, D. A. *Langmuir* **2003**, *19*, 2870–2879.
- (13) Jahn, A.; Vreeland, W. N.; Gaitan, M.; Locascio, L. E. *J. Am. Chem. Soc.* **2004**, *126*, 2674–2675.
- (14) Funakoshi, K.; Suzuki, H.; Takeuchi, S. *J. Am. Chem. Soc.* **2007**, *129*, 12608–12609.
- (15) Stachowiak, J. C.; Richmond, D. L.; Li, T. H.; Liu, A. P.; Parekh, S. H.; Fletcher, D. A. *Proc. Natl. Acad. Sci. U.S.A.* **2008**, *105*, 4697–4702.
- (16) Stachowiak, J. C.; Richmond, D. L.; Li, T. H.; Brochard-Wyart, F.; Fletcher, D. A. *Lab Chip* **2009**, *9*, 2003–2009.
- (17) Ota, S.; Yoshizawa, S.; Takeuchi, S. *Angew. Chem., Int. Ed.* **2009**, *48*, 6533–6537.
- (18) Jung, S. Y.; Retterer, S. T.; Collier, C. P. *Lab Chip* **2010**, *10*, 2688–2694.